University of Bern, Laboratory for High Energy Physics preprint BUHE-9902

To be published in the New Journal of Physics.

Impact parameter dependence of $K^{\pm}$, p, $\overline{p}$, d and $\overline{d}$ production in fixed target Pb+Pb collisions at 158 GeV per nucleon

G. Ambrosini[1], R. Arsenescu[1], C. Baglin[3], J. Beringer[1], K. Borer[1], A. Bussière[3], K. Elsener[2], Ph. Gorodetzky[5], J.P. Guillaud[3], P. Hess[1], S. Kabana[1], R. Klingenberg[1], T. Lindén[4], K.D. Lohmann[2], R. Mommsen[1], U. Moser[1], K. Pretzl[1], J. Schacher[1], F. Stoffel[1], J. Tuominiemi[4], M. Weber[1]

[1] Laboratory for High Energy Physics, University of Bern, Sidlerstrasse 5, CH-3012 Bern, Switzerland
[2] CERN, CH-1211 Geneva 23, Switzerland
[3] CNRS-IN2P3, LAPP Annecy, F-74941 Annecy-le-Vieux, France
[4] Dept. of Physics and Helsinki Institute of Physics, University of Helsinki, PO Box 9, FIN-00014 Helsinki, Finland
[5] PCC-College de France, 11 place Marcelin Berthelot, 75005 Paris, France

Abstract

Nuclear matter is expected to undergo a phase transition to quark matter in ultrarelativistic heavy ion collisions possibly showing up as a discontinuity in the impact parameter dependence of relevant observables. Following this expectation, we have investigated the impact parameter dependence of the invariant yields of $K^{\pm}$, p, d, $\overline{p}$ and $\overline{d}$ in the range $\sim$ 2 – 12 fm in fixed target Pb+Pb collisions at 158 GeV per nucleon incident energy at the CERN SPS. The particles have been measured near zero transverse momentum and in the rapidity range y=3.1 – 4.4. In addition, the centrality dependence of the baryon chemical potential, the effective temperature and the size of the particle emitting source at freeze out were studied. No dramatic change in the distribution of any of these variables is observed as a function of the impact parameter. The same is found for the particle yields, with the exception of the yield of charged kaons per number of nucleons participating in the collision (N_p), where there is an indication of a threshold behaviour at $N_p \sim 80$.

1. Introduction

The theory of quantum chromodynamics on the lattice predicts a phase transition of confined hadronic matter into deconfined quark and gluon matter at a temperature $T_c \sim$ 150-200 MeV, which could be of first order [1]. An investigation of relevant observables in heavy ion collisions as a function of energy and/or the impact parameter of the collision could signal a possible first order phase transition of the nuclear matter to quark and gluon matter (called the Quark Gluon Plasma state – QGP) through a discontinuous

behaviour of the observables at the transition point. Observation of several predicted QGP signatures (for example an increase in strange particle production, in entropy, in the volume, a suppression of J/Ψ [2]) could reveal the phase transition unambiguously.

A discontinuity in the ratio of J/Ψ over the Drell Yan production cross sections has been observed in Pb+Pb collisions at 158 GeV per nucleon at an impact parameter of $\sim$ 8 fm or at a mean number of participating nucleons $N_p \sim 140$ [3,4]. Hence it is interesting to test other QGP signatures than the J/Ψ suppression below and above this impact parameter value.

Motivated by these considerations, we have investigated the production of $K^{\pm}, p, d, \overline{p}$ and $\overline{d}$ as a function of the centrality of the collision. We have searched for sudden changes in the particle yields and in parameters like the temperature and the size of the particle source, which can be extracted from the particle yield measurements.

In searching for evidence for the QGP phase transition, it is also interesting to compare data from Pb+Pb and from hadron+nucleus collisions. This comparison can disengtangle new phenomena in heavy ion collisions. We have compared the NA52 data from Pb+Pb collisions with those from p+Be collisions at 450 GeV per nucleon [5], which were rescaled to 158 GeV per nucleon. The p+Be and Pb+Pb data presented here have both been measured using the same experimental apparatus and cover a similar phase space acceptance.

Preliminary results of this study were published in [6–9]. Results on particle and nuclei production in minimum bias Pb+Pb collisions at 158 GeV per nucleon measured in the same phase space acceptance as the results of the present paper were published in [10,11].

2. Experimental Setup

The setup of the NA52 experiment is shown in figure 1. The secondary beam line H6 in the north area of the SPS at CERN is used as a spectrometer [12]. The solid angle acceptance is $\Delta\Omega$=2.2 μsr and the momentum acceptance $\Delta p/p$=2.8%. Incident lead ions are counted with a fourfold segmented quartz Čerenkov counter (TOF0).

Particle identification is achieved by means of time of flight measurements with 5 eigthfold segmented (TOF1-TOF5) and 3 non-segmented scintillator counters (B0, B1, B2). Additional particle identification is provided by one differential (CEDAR) and 3 threshold Čerenkov counters (Č0, Č1, Č2) and a longitudinally segmented uranium/scintillator calorimeter of 7 interaction lengths (λ_{int}) placed at the end of the spectrometer. Seven multiwire proportional chambers (W1T-W5T, W2S, W3S) were used for position measurements. The charge was measured by the energy loss of the particles in the scintillation counters. The particle identification methods used in the NA52 experiment are described in references [10,11].

During the 1995 run two lead/quartz fiber electromagnetic calorimeters (QFC) of 25 radiation lengths (X_0) with pseudorapidity acceptance of $2.7 < \eta < 4.1$, positioned 0.6 m

downstream of the target were used for impact parameter selection [13,14]. The spectrometer trigger required a coincidence between the TOF2 and B1 counters. A random trigger with respect to the beam, running independently of the spectrometer trigger during the spill was also used. This trigger allowed to acquire a separate set of calorimeter data without any biases caused by the requirement of the spectrometer trigger. A 4 mm lead target, corresponding to 10% of an interaction length, was used. Empty target runs were also taken for background subtraction.

3. Centrality dependence of invariant particle yields

The invariant particle yields have been measured near zero transverse momentum and are presented as a function of the mean number of nucleons participating in the collision (N_p). This allows for a comparison with the results of other experiments measuring similar observables [3,15]. The mean number of participant nucleons in the event has been deduced by comparing the energy spectrum measured with the lead/quartz fiber calorimeter (figure 2 (a)), with the energy spectrum of $\pi^0 \rightarrow \gamma\gamma$ produced in Pb Pb collisions and simulated with the event generator VENUS 4.12 [16] in our calorimeter (figure 2 (b)). The experimentally measured energy resolution of the calorimeter was implemented in the event generator. The correspondance of the energy seen in the calorimeter and the number of participant nucleons N_p in the VENUS event generator is shown in figure 3.

The energy spectrum measured with the calorimeter was corrected for empty target interactions (see figure 2 (a)). Reinteractions in the target and δ electron contributions were expected to be small and were neglected. The energy spectrum was not corrected for the energy leakage in the calorimeter. This is taken into account in the estimation of the systematic error (see later discussion).

We have chosen five centrality regions in the measured energy distribution as indicated by lines in figure 2 (a) and numbered from 1 (the most peripheral events) to 5 (the most central events). The corresponding centrality regions in the VENUS π^0 energy spectrum have been found by demanding the integral over each centrality interval

$$\sigma_{cut} \;=\; \int_{E_{min}}^{E_{max}} \frac{d\sigma}{dE}\, dE \;. \tag{1}$$

to be the same in the data and in the simulation. The resulting cross section, the mean number of participant nucleons in the collision ($< N_p >$), and the mean impact parameter ($< b >$) of each centrality region are shown in tables 1, 2 and 3 for three different choices of energy intervals. In table 1 also the $< N_p >$ and $< b >$ for minimum bias Pb+Pb collisions taken from the VENUS event generator are shown as well as the total cross section for minimum bias Pb+Pb collisions estimated [17] from a parametrization of experimental data taken from reference [18]. This centrality determination method does not depend on the absolute energy scale. The standard deviations (σ) of the distributions of the impact parameter and the number of participants in each centrality region are given in tables 1, 2 and 3.

The invariant differential particle yields have been corrected for empty target contributions. This correction is seen to decrease with the centrality. The particle yields have been further corrected for absorption of incident ions in the target, for the spectrometer acceptance, for losses due to decay, for elastic and inelastic interactions in the beamline, for particle absorption in the target, and for the reconstruction efficiency. Pile up effects in the incident ion counting were estimated and corrected for by using the pulse height information of the TOF0 Čerenkov counter signals. The yields were not corrected for reinteractions in the target. The correction for p, $\overline{p}$ originating from decays of Λ, Δ^{++}, Δ^{+}, Δ^{0}, Δ^{-} and their antiparticles were performed using VENUS 4.12.

The systematic error on the mean number of participant nucleons is estimated to be about 13%. It arises from the uncertainty in the determination of the geometrical acceptance of the calorimeter ($\sim$ 5%), from the systematic error of the absolute normalization and shape ($\sim$ 5%) and the empty target correction ($\sim$ 5%) of the energy distribution of the calorimeter as well as from differences in the shape of the distribution in the data and the simulation ($\sim$ 10%). The latter error was determined by arbitrarily adjusting the energy scale of figure 2(b) in such a way that the spectrum overlaps with the one in figure 2(a). After this adjustement the two spectra differed by less than 10% from the mean value of the two.

We also estimated the mean number of participants using the Glauber model in the way it was implemented by the experiment NA50 [3,20] as described in reference [19]. This method is based on the assumption that the transverse energy is proportional to the number of participants. This assumption does not hold for very large number of participants [19]. The prediction of the model of reference [19] is compared to the data in figure 2(a). The mean number of participants extracted from our data using the Glauber and the VENUS model differ by less than 12% from their mean value, for number of participants less than $\sim$ 250. A direct comparison of the data presented here with the data of NA50 [3] hence seems justified. Finally the VENUS model was used throughout the analysis of this paper.

The systematic error of the invariant particle yields due to uncertainties in the energy distribution measured with the calorimeter is estimated to be $\sim$ 7 %, the uncertainty due to the spectrometer acceptance is $\sim$ 15 % and the uncertainty due to the empty target contribution correction is $\sim$ 5 %. The systematic error of the cross sections integrals over the centrality intervals due to uncertainties in the energy distribution is estimated to be $\sim$ 5 %, while the uncertainty due to the empty target contribution correction is $\sim$ 5 %. The resulting total systematic error for the particle yields is $\sim$ 17% and for the cross section integrals over the centrality bins 7 %. In the figures and tables only the statistical errors are shown.

The invariant differential particle yields for each of the five centrality regions are listed in the tables 4 and 5. The transverse momentum (p_T) acceptance of the particles ranges from zero to a maximum p_T value, which is different for each rigidity and can be calculated as: $p_T(max) \sim 0.0013 \cdot p$, with p being the momentum of the particle (see reference [21]

for a discussion of the spectrometer acceptance). Figures 4, 5 and 6 show the invariant yields of p, $\overline{p}$, d and $\overline{d}$ at rapidity y=3.7 and of $K^{\pm}$ and p at y=4.4, divided by the mean number of participant nucleons (N_p) as a function of the latter. The data are shown in 5 and/or in 16 centrality bins of tables 1 and 3. The three centrality bins shown in figure 6 as closed stars are the ones listed in table 2. Due to lack of events the yields of antideuterons at rapidity=3.1 were measurable only in the first 3 centrality bins (figure 8 and table 5).

For comparison the data measured in p+Be interactions are also shown in figure 6. They were measured at 450 GeV per nucleon by the NA56 experiment using the NA52 apparatus [5]. The systematic error on the particle yields in p+Be interactions is between 5 and 10% depending on the beam momentum [5]. It is smaller as compared to the NA52 measurements, because NA56 used different beam line conditions with smaller acceptance uncertainties. The data were rescaled to 158 GeV per nucleon using the energy dependence of measured total particle muliplicities in p+p collisions [22]. The p+Be data are compared with the Pb+Pb data in the same (y/y_{beam},p_T) acceptance. The mean number of participant nucleons for p+Be collisions was estimated with VENUS 4.12 to be $\sim$ 2.3$\pm$0.1. The total cross section for p+Be interactions was taken from reference [23] to be 0.268 barn (for energy between 80 and 240 GeV). Figures 7, 8 and 9 show the $\overline{p}/p$, $\overline{d}/d$ and the K^+/K^- production yield ratios as a function of centrality.

4. Centrality dependence of the temperature and chemical potential

Under the assumption that local thermodynamic equilibrium is established in Pb+Pb collisions in the centrality region investigated, we can estimate the effective temperature (T) and the baryon chemical potential (μ_B) from the measured particle ratios using a simple thermodynamic model. According to Boltzmann statistics, the invariant differential cross sections can be written as:

$$E\,\frac{d^3\sigma}{dp^3} \;=\; \sigma_{Pb+Pb}\;E\;\frac{2S+1}{h^3}\;V\;e^{-\frac{E\;-\;\mu_B}{T}} \qquad (2)$$

with σ_{Pb+Pb} being the total cross section of Pb+Pb collisions at 158 GeV per nucleon, S the spin of the particle, μ_B the baryon chemical potential and V the volume of the particle source. Under the assumption that V is the same for all particles, one can evaluate the ratio of the chemical potential to the temperature (μ_B/T) at freeze out from the $\overline{p}/p$ and $\overline{d}/d$ cross section ratios. We assume that $\mu_{\overline{A}} = -\mu_A = -A\mu_B$, with A, $\overline{A}$ being the nucleon numbers of particles and antiparticles, respectively.

From the measured cross section ratios d/p or $\overline{d}/\overline{p}$ and from the μ_B/T determined from equation (2), assuming that we can apply this model to the d and $\overline{d}$, we can evaluate the effective temperature:

$$T = - \frac{(A_1 - A_2) m}{ln[(E \frac{d^3\sigma}{dp^3_{A_1}} / E \frac{d^3\sigma}{dp^3_{A_2}}) \frac{A_2}{A_1} \frac{2S_{A_2}+1}{2 S_{A_1}+1}] \mp (A_1 - A_2) \frac{\mu_B}{T}} \quad (3)$$

with A_1, A_2 being the mass numbers of d and p or of $\overline{d}$ and $\overline{p}$, m the nucleon mass and S the spin. The minus sign in the denominator holds for matter and the plus sign for antimatter. Knowing T one can then extract μ_B. The resulting μ_B/T extracted from the $\overline{p}/p$ and the μ_B and T from the d/p ratios at y=3.7 are displayed in figures 10 and 11 as a function of N_p. The same parameters extracted from the $\overline{d}/d$ and the $\overline{d}/\overline{p}$ ratios agree with the values shown in the figures 10 and 11 within the errors.

5. Centrality dependence of the source size

Assuming that at y=3.7 deuterons are created by nucleon coalescence rather than by projectile fragmentation and that the phase space distributions of n and $\overline{n}$ is similar to that of the p and $\overline{p}$, it follows that the ratio of deuteron yield to the square of the proton yield ($\frac{d}{p^2}$) (same for antiparticles) give a measure of the probability that nucleons coalesce to form a deuteron. This probability depends on the nucleon distributions in phase space and in the configuration space, since only nucleons near to each other and with similar momentum can coalesce to a nucleus. The probability for the nucleons to be close enough to form a deuteron is for a given number of initial nucleons inversely proportional to the volume of the particle source. Therefore the d/p^2 and $\overline{d}/\overline{p}^2$ ratios are inversely proportional to the volume of their source.

Figure 12 shows the d/p^2 and $\overline{d}/\overline{p}^2$ ratios in Pb+Pb collisions at 158 GeV per nucleon at y=3.7 and near zero p_T. The ratios are found to decrease with increasing number of participating nucleons reflecting the increasing source size. This behaviour is in qualitative agreement with the centrality dependence of the same yield ratios measured in Si+A reactions at 11 GeV per nucleon [24]. The d/p^2 and $\overline{d}/\overline{p}^2$ ratios are combatible within the errors. Furthermore we can extract the size of the source from the d/p^2 and $\overline{d}/\overline{p}^2$ ratios using a coalescence model. The model used for the calculation of the source size ([25,26]) assumes local thermal equilibrium and uses a gaussian shape to describe the nucleon density distribution in space. The root mean square radius of the source in the rest frame of the proton and the neutron is given by:

$$R = [\frac{3}{4} \pi^{\frac{3}{2}} (\frac{h}{2\pi})^3 \frac{m_d}{m_p^2} \frac{(E \frac{d^3N}{dp^3})^2_p}{(E \frac{d^3N}{dp^3})_d} \frac{A_{Pb} - Z_{Pb}}{Z_{Pb}}]^{1/3} \quad (4)$$

where m_d, m_p are the masses of the d and p or $\overline{d}$ and $\overline{p}$, respectively. The factor $\frac{A_{Pb}-Z_{Pb}}{Z_{Pb}}$, with A_{Pb} and Z_{Pb} being the nucleon and atomic numbers of lead nucleus, accounts for the difference in the proton and neutron number in the lead nuclei, which however may change in the final state of the collision through interactions. This correction factor increases the radii by $\sim 15\%$.

Figures 13 and 14 show the calculated source radii without (figure 13) and with (figure 14) corrections for p or $\overline{p}$ coming from Λ, $\overline{\Lambda}$, Δ and $\overline{\Delta}$ decays. In figure 13 (a) we also show the results when 16 centrality bins are used (open stars). The closed star point at N_p=103 in figure 13 is extracted from the minimum bias Pb+Pb data sample. As is seen from figure 14 the particle and antiparticle data both give a source radius of $\sim$ 6.5 fm for the most central events, after corrections for the Λ, $\overline{\Lambda}$ decays. An additional correction for the Δ decays decreases the radii to about 4 fm. However, it is unclear whether part of the nucleons originating from Δ decays could contribute also to the formation of deuterons. An additional uncertainty comes from the Δ and Λ resonance production model used in the VENUS event generator. Experimental Λ production [27] comes out to be $\sim$ 40% larger than VENUS. We did not use the experimental data for this correction since they are still preliminary. In order to study the N_p dependence of the source radius and to compare it with model predictions [28,29] we parametrized the radius as $R \propto N_p^{\alpha}$ and fitted this function to the data points in the figures 13 and 14, whith α as a free parameter. The results of the fit are shown in table 6.

6. Discussion

The $\overline{d}$ yields increase towards midrapidity independent of centrality as expected. The production of $\overline{p}$ and $\overline{n}$ and therefore of $\overline{d}$ is largest near y_{cm}, where the available energy for antiparticle production has a maximum. The same trend is observed for $\overline{p}$ and $\overline{d}$ in minimum bias Pb+Pb collisions at 158 GeV per nucleon [10].

The proton and deuteron invariant yields at rapidity 3.7 increase almost linearly with the mean number of participant nucleons N_p (figures 4, 5). One would expect that protons increase linearly or slightly more than linearly with N_p, since most of the protons are inherited from the participating protons of the lead nuclei and only a small part is due to direct p and $\overline{p}$ production. The expectation for the centrality dependence of deuterons is less straightforward, since their production through coalescence may depend also on other parameters than N_p.

The $\overline{p}$ and $\overline{d}$ yields divided by the number of participant nucleons N_p shown in figures 4 and 5 decrease with increasing N_p. This behaviour, as well as the decrease of the $\overline{p}/p$ and the $\overline{d}/d$ yield ratios with increasing centrality (figures 7 and 8) indicates larger $\overline{p}$ and $\overline{d}$ absorption with higher baryon density.

The K^+/K^- ratio at y=4.4 does not change significantly as a function of the centrality (figure 9). A similar behaviour of this ratio has been measured in Au+Au collisions at 10.8 A GeV [30].

There is an indication of a deviation from a linear behaviour in the $K^{\pm}/N_p$ ratio shown in figure 6 in the region below $N_p \sim 80$. The observation of a nearly linear behaviour above $\sim$ 80 N_p could be interpreted as an onset of equilibration of kaons. This however seems to be more pronounced with K^+ than with K^-. The K^+/N_p and K^-/N_p ratios

in p+Be collisions (also shown in figure 6) are smaller than those of central Pb+Pb collisions. This is in agreement with similar results of other experiments [31–33].

The measured effective temperature for the most central Pb+Pb collisions is 126±5 MeV after correcting for protons coming for decays (figure 10). This temperature characterizes the chemical freeze-out of the deuterons and protons, meaning that after that time, deuterons and protons do not change their identity through further collisions. This value is smaller than the temperature of $\sim$ 170 MeV characterizing the chemical freeze-out of hadrons in full phase space acceptance in central S+A and Pb+Pb collisions at 200 and 158 GeV per nucleon determined in the framework of thermodynamical models using measured particle yield ratios ([34,35]).

The difference in temperature between the value obtained from our analysis using deuteron and proton yields and the one using ratios of hadrons (π, K etc.) in other experiments ([34,35]), could be due to the limited phase space acceptance of our spectrometer and/or to the fact that deuterons and antideuterons are mainly formed at a later stage of the collision than hadrons. One would expect that nuclei form at the time of thermal freeze out of hadrons, since they can easily be destroyed in elastic collisions with other particles, due to their weak binding. The thermal freeze-out is meant as the time after which the hadrons do not interact anymore, through both elastic or inelastic collisions. The temperature of the thermal freeze out extracted from fits to the m_T spectral shapes of the hadrons as well as from $\pi\pi$ interferometry are of the order of $\sim$ 120 MeV [37]. Consequently the chemical freeze out of hadrons occurs at a higher temperature and therefore earlier than the thermal freeze out. The similarity of the temperature obtained in this study from the d/p ratios in central Pb+Pb events and the temperature of the thermal freeze out obtained from spectral shapes and correlations of hadrons, supports the assumption that d and $\overline{d}$ are formed mainly at a later stage of the collision than hadrons, namely at the time of the thermal freeze-out of the latter.

The radius of the baryon source extracted from the d/p^2 ratio increases as $R \sim N_p^{0.32-0.38}$, and the one of the antibaryon source (extracted from the $\overline{d}/\overline{p}^2$ ratio) as $R \sim N_p^{0.38-0.43}$ (figures 13 and 14), depending on the decay correction applied. In reference [29] the assumption that freeze out occurs at a common constant critical density leads to the expectation $R \sim (N_p)^{1/3}$, assuming that N_p is proportional to the rapidity density of the charged hadrons at midrapidity. This assumption is supported by the scaling of the π^- to N_p ratio with N_p, observed in heavy ion collisions [36,38]. The same dependence holds for radii of nuclei ($R = 1.2A^{1/3}$ fm). Assuming that the freeze out occurs when the mean free path of the particles becomes similar to the radius of the particle source, a dependence of $R \sim (N_p)^{\frac{1}{2}}$ is expected [28]. The N_p dependence of the source radius extracted in this study from the d/p^2 yield ratio is in agreement with the expectation $R \sim (N_p)^{\frac{1}{3}}$. The source radii extracted from the $\overline{d}/\overline{p}^2$ ratio can not discriminate between the two predictions.

The particle source size in central Pb+Pb collisions at 158 GeV per nucleon has also been deduced from two particle (e.g. $\pi\pi$) correlation analysis [39,37]. The radii extracted

from $\pi\pi$ interferometry in Pb+Pb collisions at 158 GeV per nucleon, at the same y and p_T as the NA52 data and for $N_p \sim 360$, are found to be $R_T \sim 6$ fm and $R_L \sim 8$ fm, were R_T is the transverse and R_L the longitudinal radius calculated in the longitudinally comoving system [37]. These radii are not corrected for π yields from resonance decays, however this correction is predicted to reduce the radius at zero p_T by less than 10% [40]. Since resonance decays affect much more the results of the coalescence method (R_{COAL}) than those of $\pi\pi$ correlation method ($R_{\pi\pi}$), it seems reasonable to compare the decay corrected R_{COAL} to the uncorrected $R_{\pi\pi}$ values. Furthermore, since the deuteron, nucleon and pion freeze out mechanisms may differ, the extracted source sizes could be different.

If the particle source was a non expanding thermal source, the radius extracted from the d/p^2 ratio would be an estimate of the root mean square radius of the source. However there is experimental evidence that the particle source in Pb+Pb collisions at 158 GeV per nucleon expands considerably and a collective motion is superimposed on the thermal motion of the particles (e.g. [41,37]). Therefore positions and momenta of the particles are correlated and the measured radii are effective values, smaller than the real source dimensions. As a result of the collective source expansion, the effective radius is a decreasing function of the transverse mass m_T ($m_T = \sqrt{p_T^2 + m^2}$) [41].

In figure 15 the results for the source size extracted from $\pi\pi$ correlations [42] are compared to those obtained from this analysis as a function of m_T. The measurements are done at a similar rapidity and similar number of participating nucleons. The line in figure 15 indicates the fit of the function $R = c(1 + m_T\beta)^{-1/2}$ to the data points shown as stars with c and β free parameters in the fit. This dependence is expected for a collective expanding source [41]. Our results are seen to be consistent with the $R_{\pi\pi}$ radii within this picture, after correcting for the Δ and Λ decays and without the correction for the neutron/proton asymmetry in lead.

7. Conclusions

Results on the impact parameter dependence of the $K^{\pm}$, p, d, $\overline{p}$ and $\overline{d}$ invariant differential yields in Pb+Pb collisions at 158 GeV per nucleon near zero transverse momentum, at rapidities 3.1 to 4.4 and in the impact parameter range from $\sim$ 2 to 12 fm have been presented.

The centrality dependence of the antibaryon yields indicates absorption at high baryon density. In the K^+/N_p and K^-/N_p ratios at y=4.4 there is an indication of a threshold behaviour, the ratios rising faster than linear with N_p up to $N_p \sim 80$ and saturating above that value. It is however unclear, whether this can be related to a QGP phase transition or it reflects the onset of thermalization in a hadron gas. The low freeze-out effective temperature of 126 MeV measured in this analysis in the most central events may be related to the late formation of d and $\overline{d}$ through coalescence.

The radius of the particle emitting source extracted from the d/p^2 and $\overline{d}/\overline{p}^2$ ratios is found to be $\sim$ 4 fm for central events near y_{cm}, after correcting for decays of Δ and Λ. The

low value of this radius as compared to the source size measured using $\pi\pi$ correlations at similar y and centrality [42] can be understood within a picture of a collective expanding source [41]. The increase of the source radius with N_p is compatible with $R \propto (N_p)^{\frac{1}{3}}$. No sudden change of the chemical potential, the temperature or the radius of the source has been observed.

Acknowledgments

We thank Prof. U. Heinz and Prof. P. Minkowski for fruitful discussions. We also thank Dr. C. Lourenco, Dr. N. Carrer and Dr. M. Nardi for their help concerning the application of the method used by the NA50 and WA97 experiments for the extraction of the number of participants to the NA52 data.

REFERENCES

1. E. Laermann, Quark Matter '96 Proc., Nucl. Phys. A 610 (1996) 1c.
2. S. A. Bass et al., hep-ph/9810281, submitted to J. Phys. G.
3. M.C. Abreu et al., (NA50 coll.), Phys. Lett. B 410 (1997) 337.
4. J.Y. Ollitrault, private communication.
5. G. Ambrosini et al. (NA56 Coll.), submitted to European Journal of Phys. C.
6. S. Kabana et al.(NA52 coll.), Journal of Phys. G: Nuclear and Particle Physics, 23 (1997) 2135.
7. S. Kabana et al.(NA52 coll.), Nucl. Phys. A 638 (1998) 411c.
8. S. Kabana et al.(NA52 coll.), Journal of Phys. G: Nuclear and Particle Physics, Vol. 25, Nr. 2, (1999) 217.
9. S. Kabana et al. (NA52 coll.), contribution to the International Conference on Quark Matter, 10-15 May 1999, Torino, Italy, to be published in the proceedings.
10. G. Ambrosini et al. (NA52), Phys. Lett. B 417 (1998) 202.
11. G. Appelquist et al. (NA52), Phys. Lett. B 376 (1996) 245.
12. K. Pretzl et al (NA52 coll.), Proc. of the Int. Symp. on Strangeness and Quark matter, World Scientific (1995) 230.
13. M. Weber et al (NA52 Coll.), Proceedings of the VII International Conference on Calorimetry in High Energy Physics, 9-14 Nov. 1997, Tucson, Arizona, USA, Proceedengs edited by E. Cheu et al., World Scientific Publishing Co. Pte. Ldt. (1998) 151, Univ. of Bern preprint BUHE-97-10.
14. M. Weber, Diploma Thesis, University of Bern, 1996, http://www.lhep.unibe.ch/newmass/publications/theses/theses.html.
15. E. Andersen et al., (WA97 coll.), CERN-EP/99-29, submitted to Phys. Lett. B.
16. K. Werner, Phys. Rep. 232 (1993) 87.
17. F. Stoffel, Ph. D. Thesis, University of Bern 1997, http://www.lhep.unibe.ch/newmass/publications/theses/theses.html.
18. E. Andersen et al., (NA36 coll.) Phys. Lett. B 220 (1989) 328.
19. D. Kharzeev et al., CERN-TH/96-328.

20. C. Lourenco, private communication.
21. R. Klingenberg, Ph. D. Thesis, University of Bern, March 1996, http://www.lhep.unibe.ch/newmass/publications/theses/theses.html.
22. E. Albini et al., Nucl. Phys. B 84 (1975) 269.
23. Review of Particle Properties, Physical Review D Particles and Fields Vol. 50 (1994) 1241.
24. J. Barrette et al., (E814 Coll.), Phys. Rev. C 50, 2 (1994) 1077, L. Ahle et al., (E802 Coll.) Phys. Rev. C 50, 2 (1994) 1024.
25. W.J. Llope et al., Phys. Rev. C 52, (1995) 4.
26. B. Holzer et al. (NA44), 13th Winter Workshop on Nucl. Dynamics, Florida, 1-8 Feb 1997.
27. P. Jones et al. (NA49 coll.), Nucl.Phys. A 610 (1996) 188c.
28. R.Stock Ann. der Phys. 48 (1991) 195.
29. I. Pomeranchuk, Dokl. Akad. Nauk. SSSR78, (1951) 884.
30. Y. Akiba et al. (E866 coll), Nucl. Phys. A 610 (1996) 139c.
31. T. Alber at al., (NA35 Coll.), Z. Phys. C 64 (1994) 195.
32. G. Roland et al. (NA49 Coll.), Nucl. Phys. A 638 (1998) 91c.
33. P.Seyboth, Journal of Physics G: Nuclear and Particle Physics, Vol. 23 Number 12 (1997), 1787.
34. P.Braun Munzinger and J. Stachel, Nucl. Phys. A 638 (1998) 3c.
35. F. Becattini et al., Nucl. Phys. A 638 (1998) 3c.
36. H. Appelshäuser et al. (NA49 Coll.), nucl-ex/9810014, submitted for publication.
37. H. Appelshauser et al. (NA49 coll.), Eur. Phys. J. C2 (1998) 661.
38. T. Alber et al. (NA35 coll.), Eur. Phys. J. C2 (1998) 643.
39. A. Sakaguchi et al. (NA44 Coll.), Nucl. Phys. A 638 (1998) 103c.
40. U. Heinz, Nucl.Phys. A 610 (1996) 264c.
41. U. Heinz and R. Scheibl, nucl-th/9809092, submitted for publication.
42. H. Appelshäuser, Ph. D. Thesis, University Frankfurt am Main, 1997.

centrality cut	σ_{cut} (barn)	$< N_p >$	$< b >$ (fm)
no cut	8.2 ± 2.0	103 ± 2	10.25 ± 0.09
1	2.483 ± 0.034	62.5 ± 0.5 (41.7)	11.00 ± 0.02 (1.7)
2	1.379 ± 0.019	149.3 ± 0.9 (58.7)	8.15 ± 0.02 (1.6)
3	0.835 ± 0.013	236.8 ± 1.2 (63.6)	5.81 ± 0.03 (1.7)
4	0.505 ± 0.010	297.8 ± 1.3 (55.5)	4.13 ± 0.04 (1.6)
5	0.253 ± 0.001	336.3 ± 1.6 (42.6)	3.02 ± 0.05 (1.4)

Table 1
Cross section σ_{cut}, mean number of participant nucleons in the collision $< N_p >$ and mean impact parameter $< b >$ for the five centrality bins illustrated in figure 2 and used in the tables 4 and 5 as well as in most figures. σ_{cut} is the cross section of each centrality region, defined as $\sigma_{cut} = \int_{Emin}^{Emax} \frac{d\sigma}{dE} dE$. The first line of the table corresponds to minimum bias Pb+Pb collisions (no centrality cut) and the corresponding cross section has been estimated [17] from a parametrization of experimental data taken from reference [18]. The errors shown are the statistical errors, while the values in parenthesis are the standard deviations of the distributions of N_p and b in the considered centrality ranges.

centrality cut	$< N_p >$	$< b >$ (fm)
1	36.6 ± 0.6 (27.2)	12.12 ± 0.03 (1.5)
2	47.2 ± 0.8 (31.4)	11.56 ± 0.04 (1.4)
3	58.8 ± 1.0 (34.0)	11.07 ± 0.04 (1.4)

Table 2
Mean number of participants $< N_p >$ and mean impact parameter $< b >$ for the 10 GeV wide bins in energy, shown with closed stars in figure 6. The errors shown are the statistical errors. The values in parenthesis are the standard deviations of the distributions of N_p and b in the considered energy interval.

centrality cut	$< N_p >$	$< b >$ (fm)
1	45.4 ± 0.5 (31.6)	11.75 ± 0.04 (0.83)
2	81.1 ± 0.8 (40.7)	10.49 ± 0.04 (0.75)
3	110.6 ± 1.1 (47.3)	9.36 ± 0.04 (0.70)
4	143.0 ± 1.4 (53.1)	8.64 ± 0.05 (0.71)
5	166.5 ± 1.6 (55.1)	7.86 ± 0.05 (0.62)
6	193.6 ± 1.7 (58.3)	7.12 ± 0.06 (0.63)
7	217.1 ± 2.0 (60.9)	6.61 ± 0.07 (0.71)
8	242.6 ± 2.1 (59.3)	5.90 ± 0.07 (0.77)
9	266.4 ± 2.2 (60.3)	5.28 ± 0.07 (0.73)
10	282.2 ± 2.3 (56.3)	4.95 ± 0.07 (0.62)
11	294.6 ± 2.4 (55.2)	4.55 ± 0.09 (0.88)
12	317.3 ± 2.4 (49.6)	3.63 ± 0.10 (0.75)
13	324.1 ± 2.3 (44.1)	2.69 ± 0.12 (0.92)
14	340.2 ± 2.5 (39.2)	2.61 ± 0.16 (1.06)
15	340.2 ± 3.6 (44.1)	2.02 ± 0.16 (0.96)
16	351.7 ± 3.6 (33.3)	2.25 ± 0.20 (0.65)

Table 3
Mean number of participants $< N_p >$ and mean impact parameter $< b >$ for the 30 GeV wide bins in energy, shown with open stars in figures 6 and 13, respectively with open triangles in figure 4. The values in parenthesis are the standard deviations of the distributions of N_p and b in the considered energy intervals.

centrality cut	$2\pi E\frac{d^3N}{dp^3}$ (GeV^{-2})	$2\pi E\frac{d^3N}{dp^3}$ (GeV^{-2})	$2\pi E\frac{d^3N}{dp^3}$ (GeV^{-2})
	p y=3.7 uncorrected for decays	p y=3.7 corrected for Λ decay	p y=3.7 corrected for Λ, Δ decay
1	11.70 ± 0.49	8.81 ± 0.42	5.01 ± 0.24
2	30.09 ± 0.95	22.90 ± 0.82	12.22 ± 0.44
3	44.07 ± 1.40	33.27 ± 1.19	16.92 ± 0.62
4	61.43 ± 2.11	46.44 ± 1.75	22.98 ± 0.88
5	71.26 ± 3.06	53.80 ± 2.52	26.29 ± 1.25
	p y=4.4	p y=4.4 corrected for Λ decay	p y=4.4 corrected for Λ, Δ decay
1	18.45 ± 0.74	13.89 ±0.64	7.89 ± 0.36
2	43.72 ± 1.34	33.27 ± 1.17	17.75 ± 0.63
3	60.96 ± 1.87	46.03 ± 1.62	23.41 ± 0.83
4	77.28 ± 2.58	58.42 ± 2.16	28.90 ± 1.08
5	78.29 ± 3.26	59.11 ± 2.70	28.89 ± 1.34
	$\overline{p}$ y=3.7 uncorrected for decays	$\overline{p}$ y=3.7 corrected for $\overline{\Lambda}$ decay	$\overline{p}$ y=3.7 corrected for $\overline{\Lambda}$, $\overline{\Delta}$ decay
1	0.937 ± 0.038	0.529 ± 0.038	0.287 ± 0.021
2	2.041 ± 0.064	1.059 ± 0.059	0.551 ± 0.033
3	2.586 ± 0.082	1.290 ± 0.074	0.621 ± 0.041
4	3.375 ± 0.116	1.707 ± 0.097	0.837 ± 0.052
5	3.752 ± 0.162	1.932 ± 0.131	0.938 ± 0.069

Table 4
Invariant differential particle yields in Pb+Pb collisions at 158 GeV per nucleon, near zero transverse momentum, as a function of rapidity and centrality. The Λ and Δ decay corrections have been performed using VENUS 4.12 [16].

centrality cut	$2\pi E\frac{d^3N}{dp^3}$ (GeV^{-2})	$2\pi E\frac{d^3N}{dp^3}$ (GeV^{-2})	$2\pi E\frac{d^3N}{dp^3}$ (GeV^{-2})
	d y=3.1	d y=3.7	$\overline{d}$ y=3.1
1	0.028 ± 0.009	0.058 ± 0.011	$(8.01 \pm 4.06)10^{-4}$
2	0.081 ± 0.017	0.134 ± 0.018	$(6.33 \pm 3.83)10^{-4}$
3	0.119 ± 0.025	0.196 ± 0.027	$(7.32 \pm 5.15)10^{-4}$
4	0.188 ± 0.041	0.282 ± 0.042	
5	0.171 ± 0.060	0.200 ± 0.054	
	$\overline{d}$ y=3.7	K^+ y=4.4	K^- y=4.4
1	$(3.00 \pm 0.94)10^{-4}$	10.39 ± 0.72	6.29 ± 0.25
2	$(2.97 \pm 0.99)10^{-4}$	34.08 ± 1.46	17.18 ± 0.54
3	$(2.57 \pm 1.15)10^{-4}$	52.27 ± 2.29	27.69 ± 0.88
4	$(5.11 \pm 2.08)10^{-4}$	75.07 ± 3.52	40.75 ± 1.39
5	$(2.03 \pm 2.12)10^{-4}$	88.74 ± 5.55	47.73 ± 2.03

Table 5
Invariant differential particle yields in Pb+Pb collisions at 158 GeV per nucleon, near zero transverse momentum, as a function of rapidity and centrality.

	$p_1(d/p^2)$ (fm)	$\alpha(d/p^2)$	$p_1(\overline{d}/\overline{p}^2)$ (fm)	$\alpha(\overline{d}/\overline{p}^2)$
	5 bins	5 bins	5 bins	5 bins
uncorrected data	0.70 ± 0.20	0.38 ± 0.05	0.55 ± 0.30	0.47 ± 0.09
corrected for Λ, $\overline{\Lambda}$ decay	0.58 ± 0.17	0.38 ± 0.05	0.43 ± 0.27	0.43 ± 0.10
corrected for Λ, $\overline{\Lambda}$ and Δ, $\overline{\Delta}$ decay	0.51 ± 0.15	0.32 ± 0.05	0.35 ± 0.22	0.38 ± 0.10
	$p_1(d/p^2)$ (fm)	$\alpha(d/p^2)$		
	16 bins	16 bins		
uncorrected data	0.77 ± 0.21	0.35 ± 0.05		

Table 6
Results of the fit of the function $R = p_1 N_p^{\alpha}$ to the radii as a function of the number of participant nucleons displayed in figures 13 and 14, with p_1 and α as free parameters.

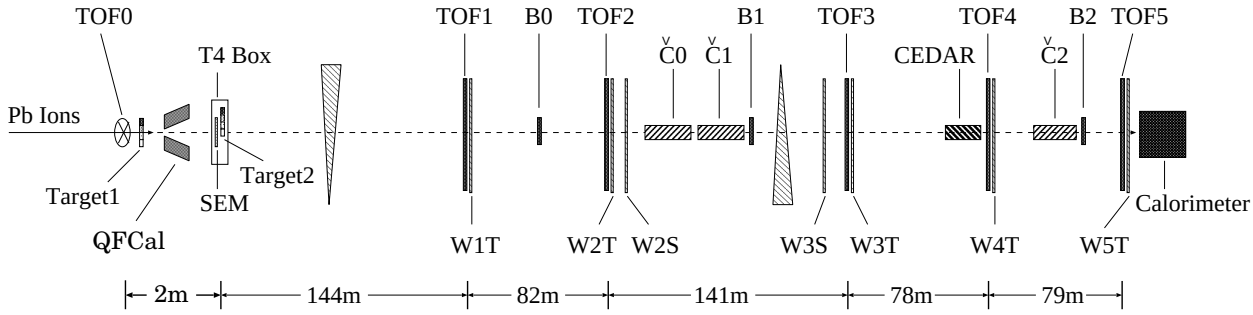

Figure 1. The NA52 experimental set-up for the 1995 run.

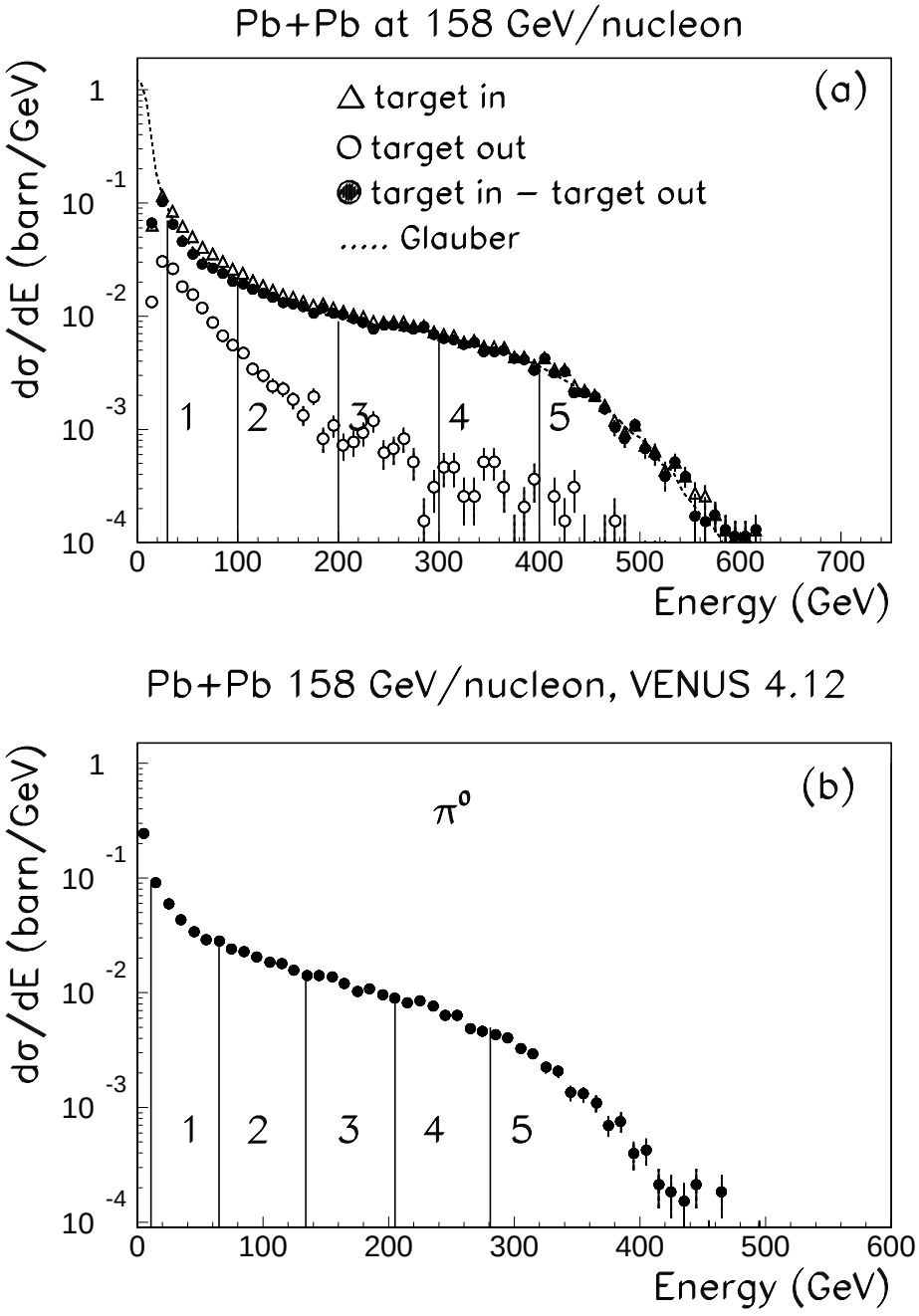

Figure 2. Cross section as a function of energy seen in the lead/quartz fiber calorimeter in Pb+Pb collisions at 158 GeV per nucleon (a). The calorimeter threshold was set at $\sim$ 20 GeV. In (b) the cross section as a function of energy for $\pi^0 \to \gamma\gamma$ produced in Pb+Pb collisions at 158 GeV per nucleon, simulated with VENUS 4.12 model [16] is shown. The lines and numbers in both distributions indicate the selected centrality regions for the analysis (for the results see table 1).

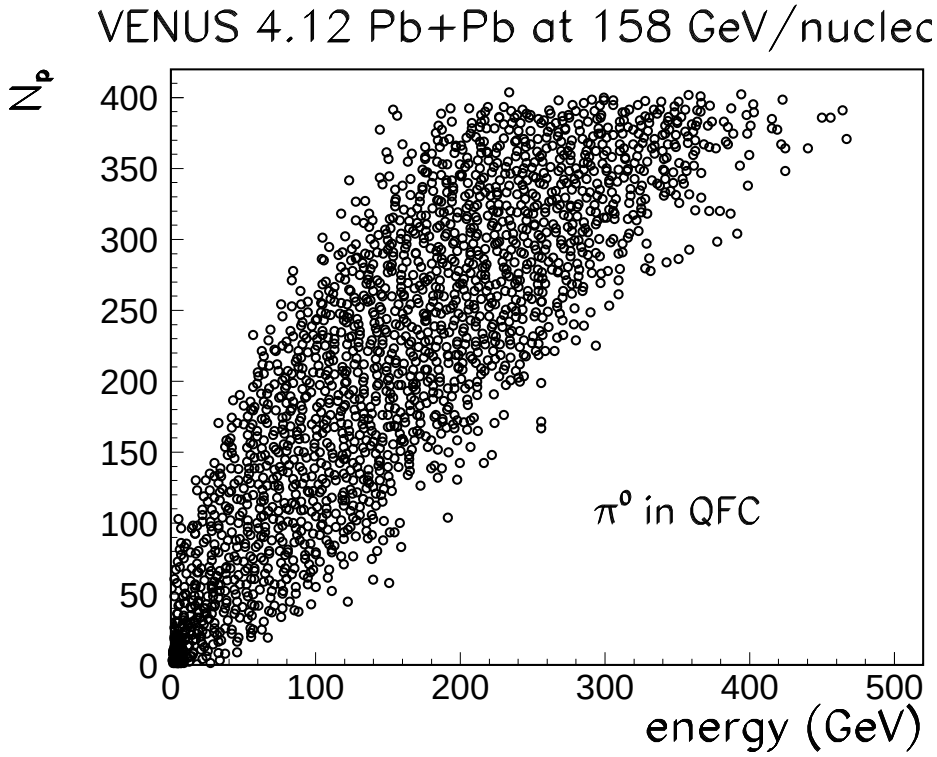

Figure 3. VENUS 4.12 simulation of the mean number of participating nucleons as a function of the energy of $\pi^0 \to \gamma\gamma$ seen in the QFC calorimeter.

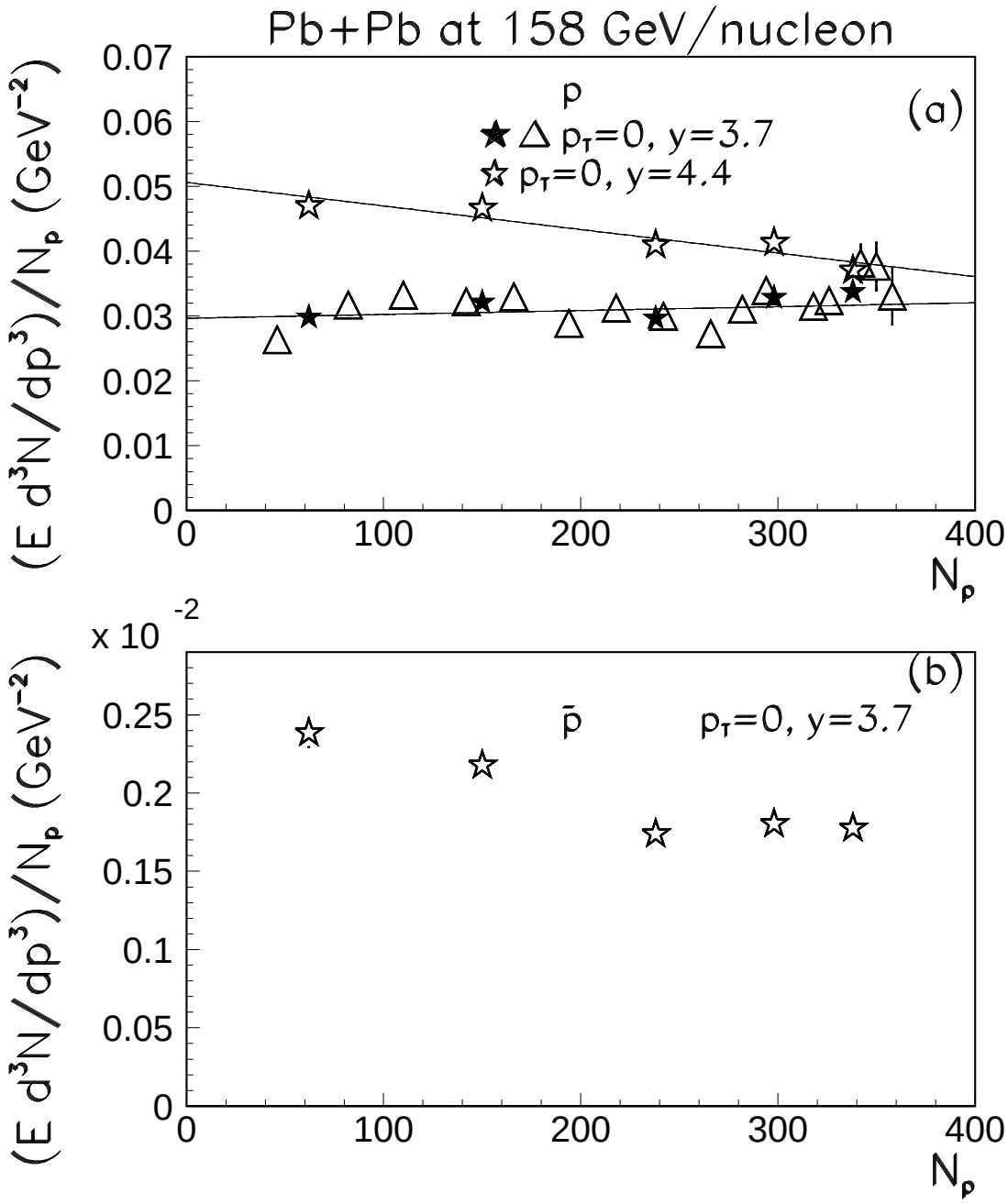

Figure 4. Invariant yields of p (a) and $\overline{p}$ (b) in Pb+Pb collisions at 158 A GeV near zero p_T and at y=3.7 and of p at y=4.4 (a) divided by the mean number of participant nucleons N_p, as a function of N_p.

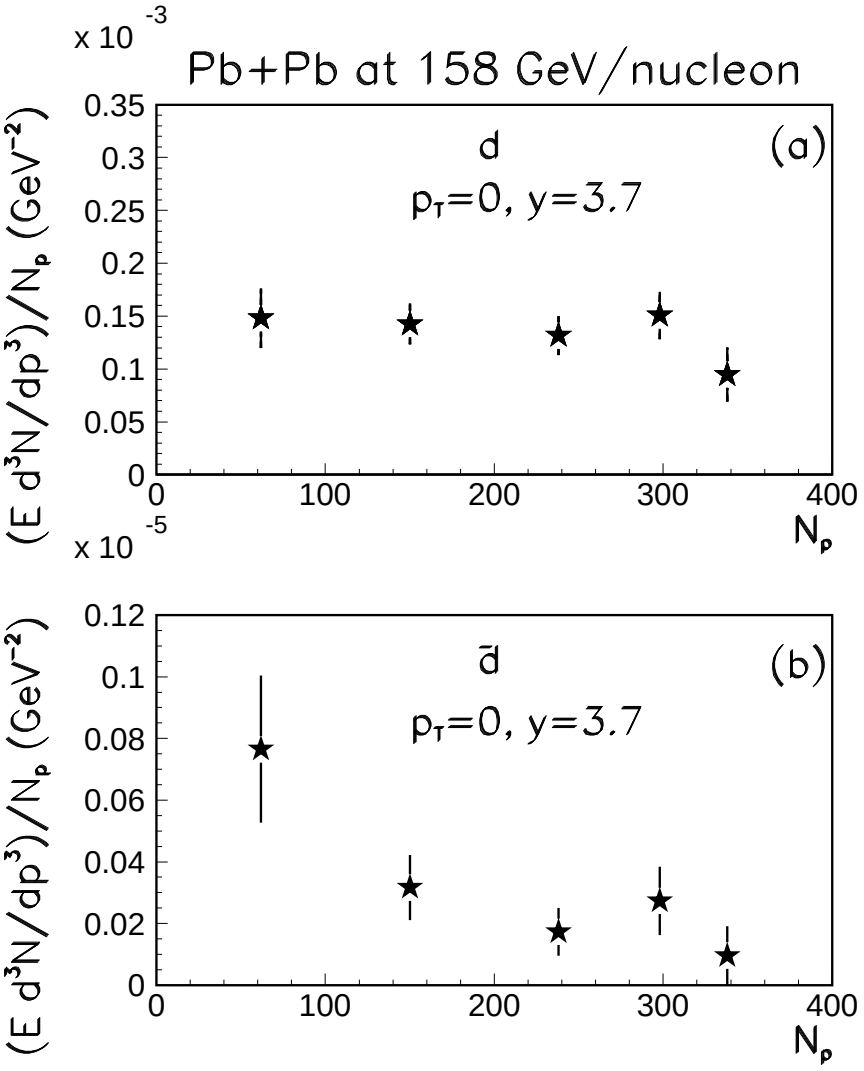

Figure 5. Invariant yields of d (a) and $\overline{d}$ (b) in Pb+Pb collisions at 158 A GeV near zero p_T and at y=3.7, divided by the mean number of participant nucleons N_p, as a function of N_p.

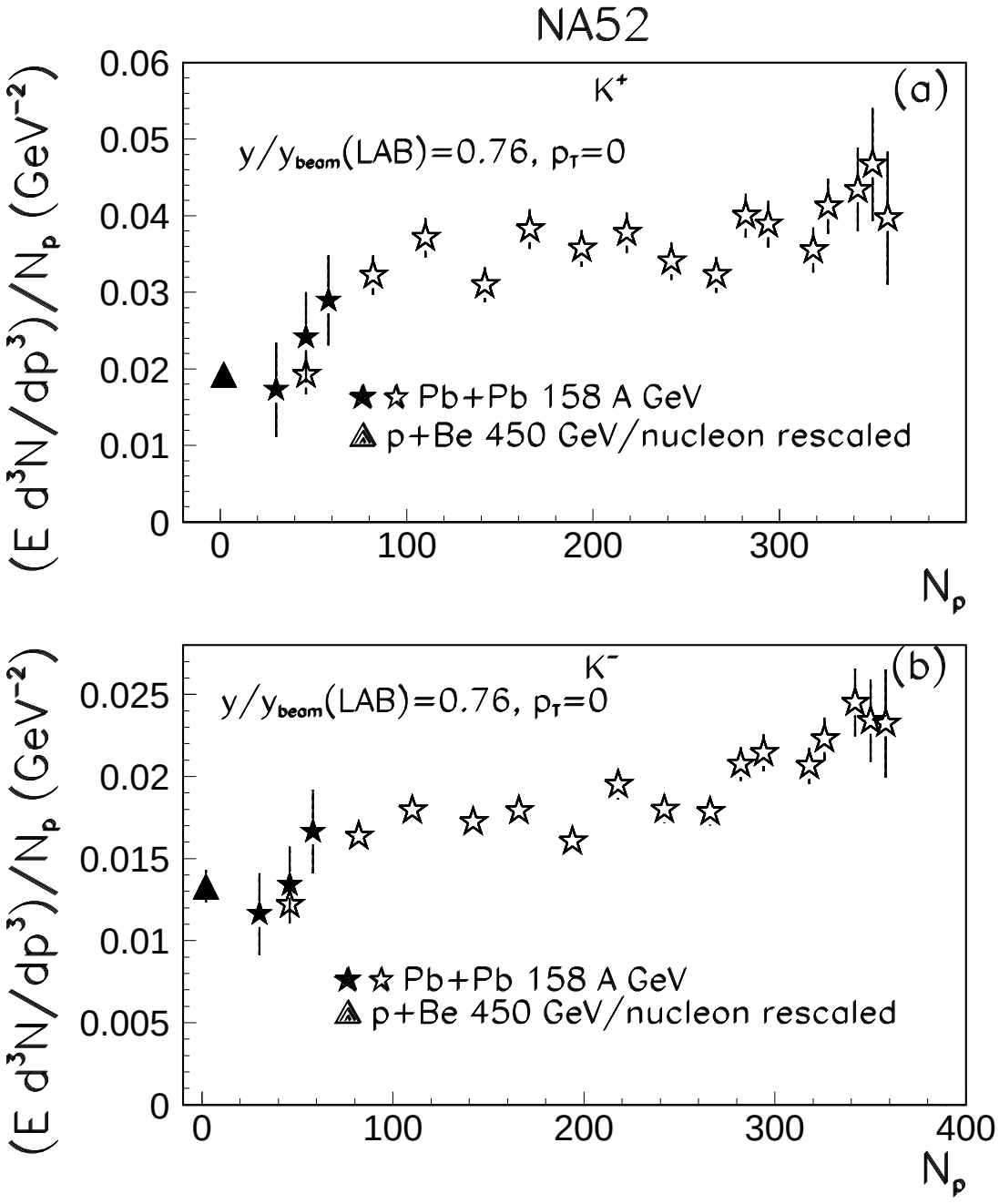

Figure 6. Dependence of the $K^{\pm}$ invariant yields in Pb+Pb collisions at 158 A GeV near zero p_t divided by the mean number of participant nucleons N_p from N_p. For comparison the data (closed stars) are also shown with a smaller bin size (see table 2). The p+Be data were measured at 450 GeV per nucleon [5] and have been rescaled to 158 GeV per nucleon (see text) and are compared to the Pb+Pb data at the same p_T and y/y_{beam}.

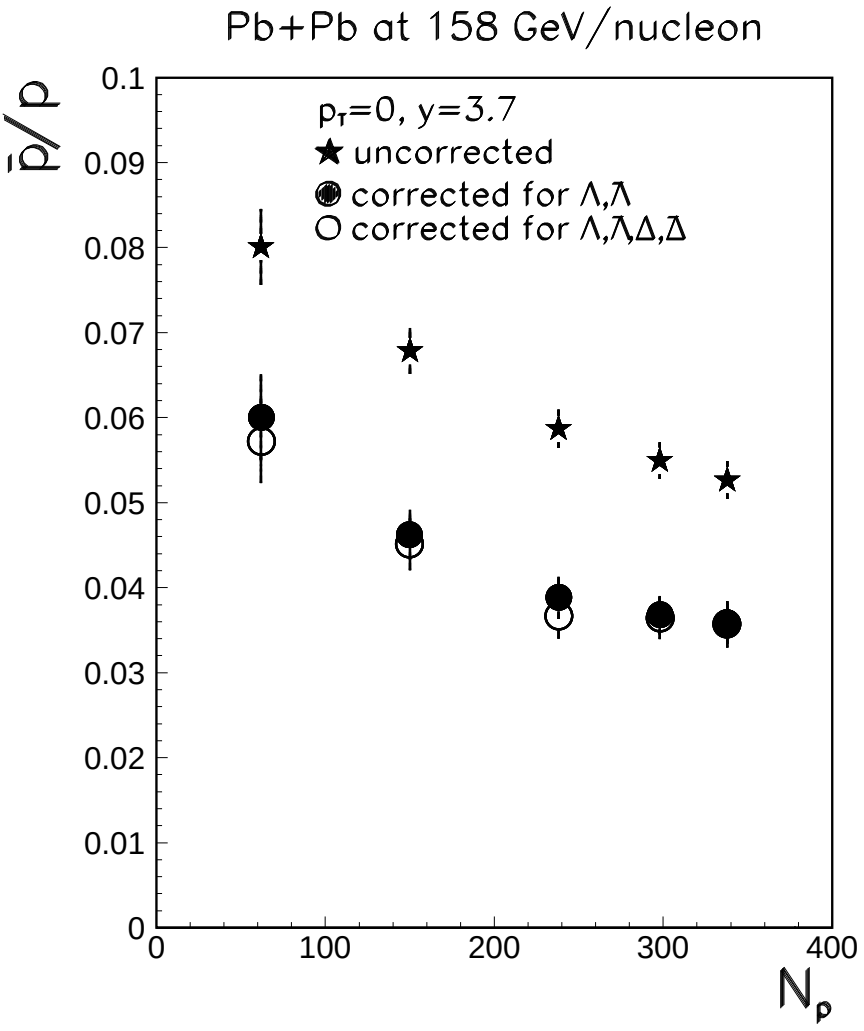

Figure 7. Dependence of the $\overline{p}/p$ ratio from the mean number of participant nucleons in Pb+Pb collisions at 158 A GeV near zero p_T and at y=3.7. The Λ and Δ correction is performed using VENUS 4.12 [16]

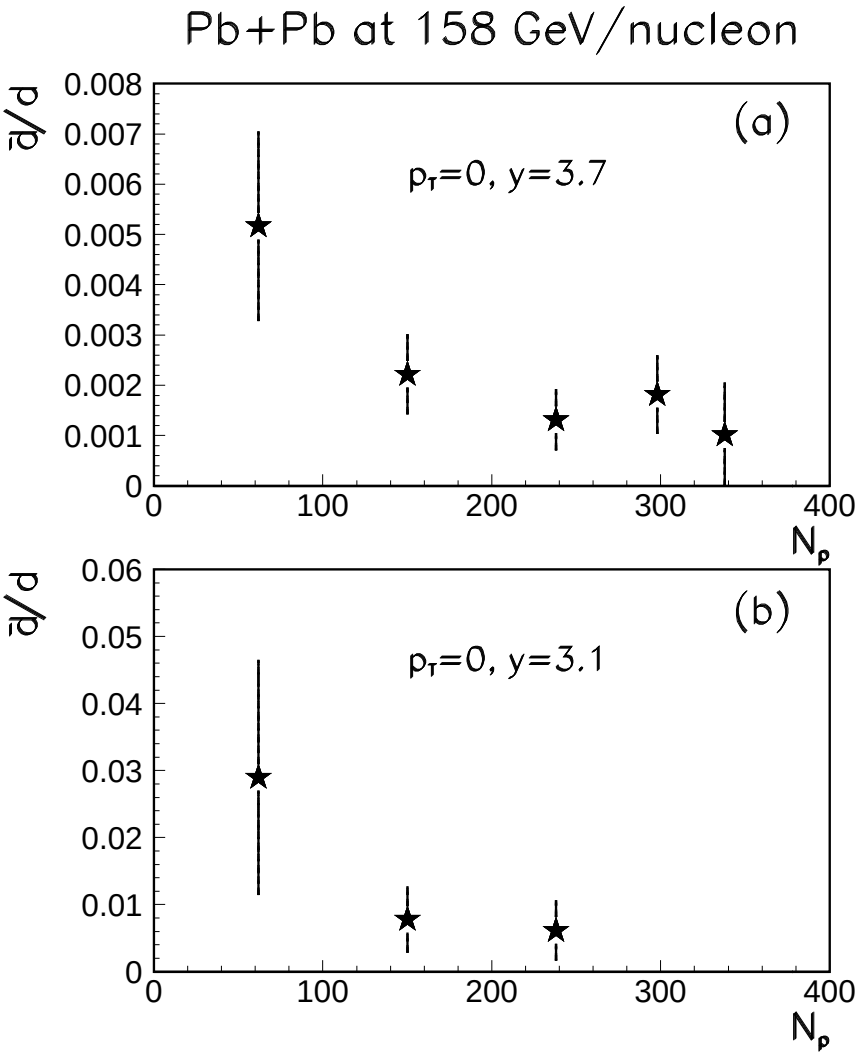

Figure 8. Dependence of the $\overline{d}/d$ ratio from the mean number of participant nucleons in Pb+Pb collisions at 158 A GeV near zero p_T and at y=3.7 (a) and y=3.1 (b).

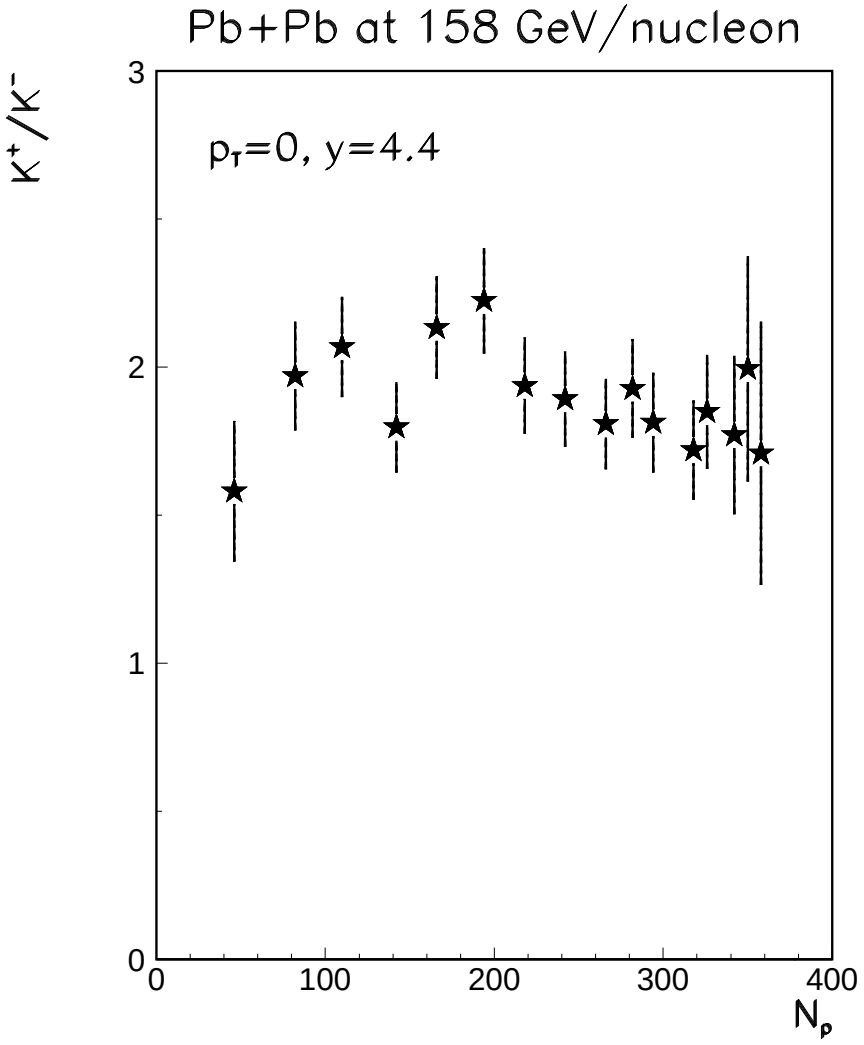

Figure 9. Dependence of the K^+/K^- ratio from the mean number of participant nucleons in Pb+Pb collisions at 158 A GeV near zero p_T and y=4.4.

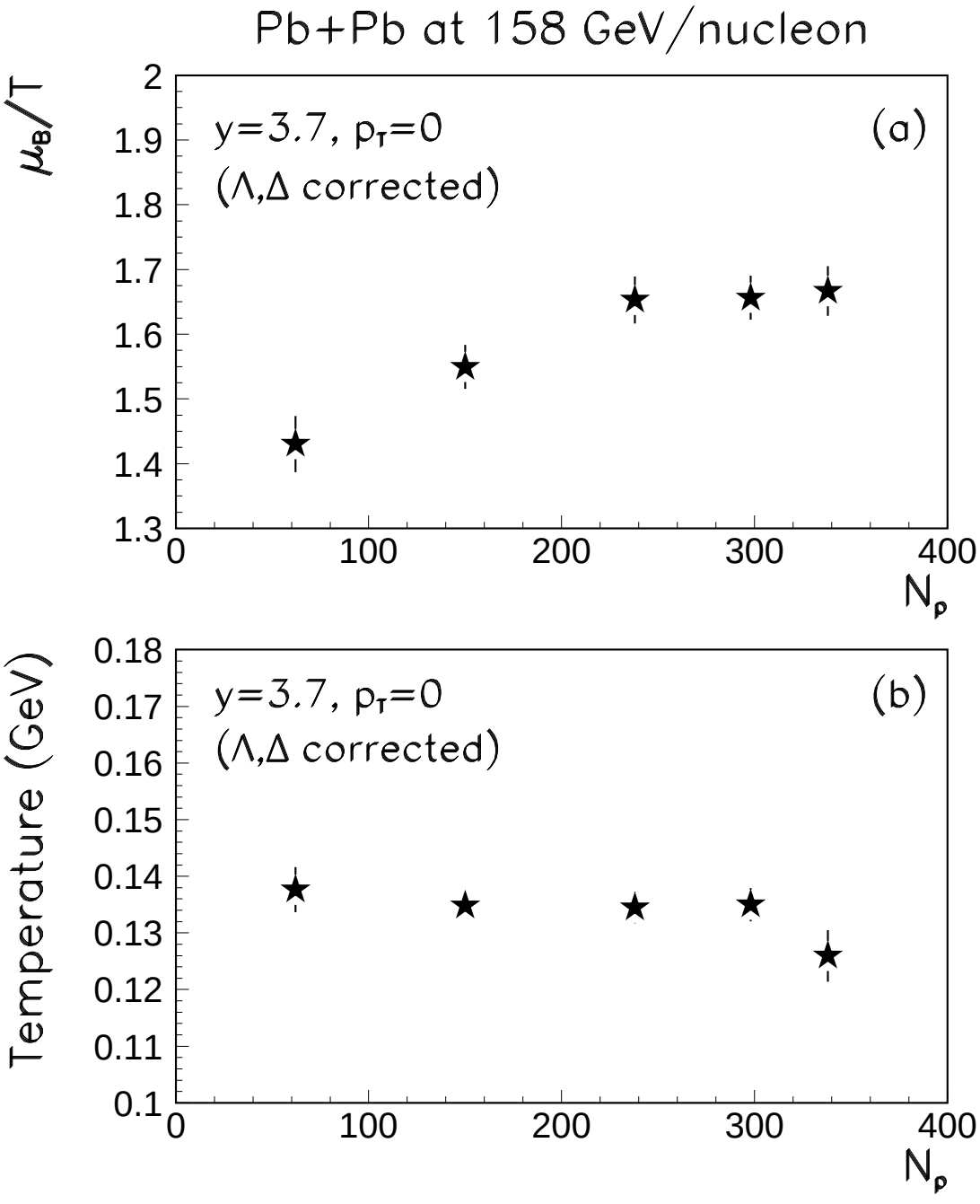

Figure 10. The baryochemical potential μ_B over the temperature T extracted from the $\overline{p}/p$ ratio (a) and the T extracted from the d/p ratio (b), at y=3.7 and near zero p_T in Pb+Pb collisions at 158 A GeV, as a function of the mean number of participant nucleons. p and $\overline{p}$ have been corrected for Λ, $\overline{\Lambda}$, Δ and $\overline{\Delta}$ decays [16].

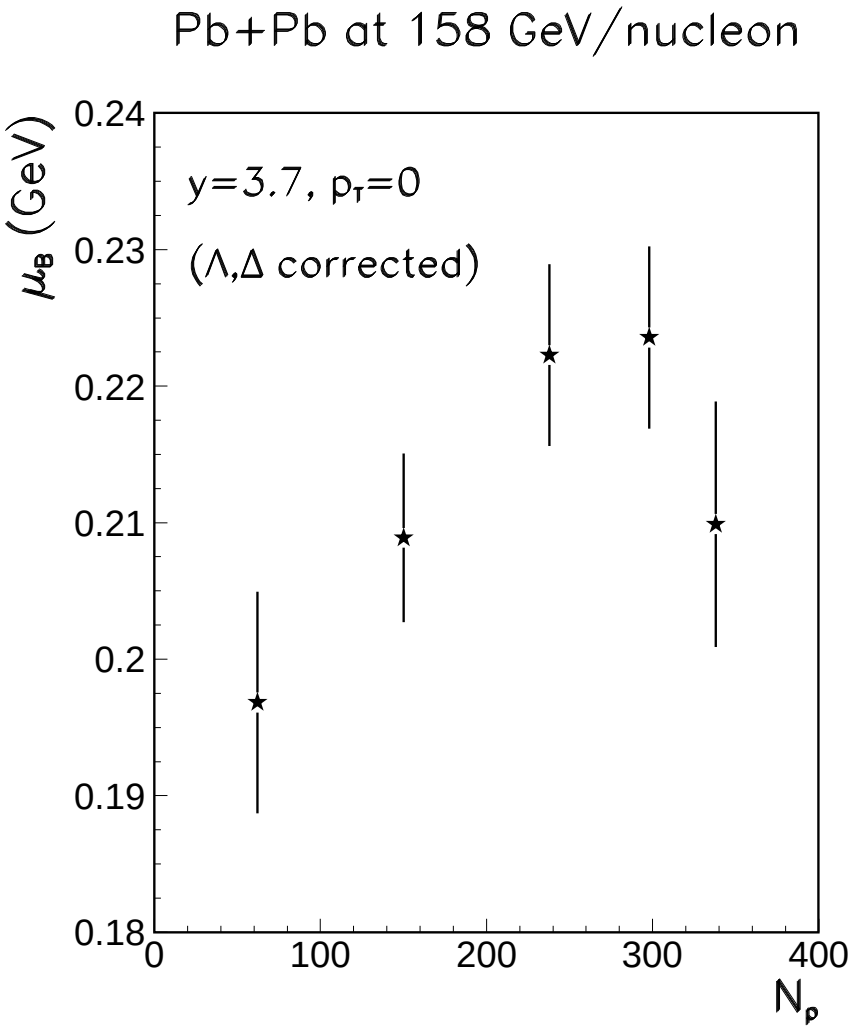

Figure 11. The baryochemical potential μ_B extracted from the μ_B/T and T values shown in figure 10 at y=3.7 and near zero p_T in Pb+Pb collisions at 158 A GeV, as a function of the mean number of participant nucleons.

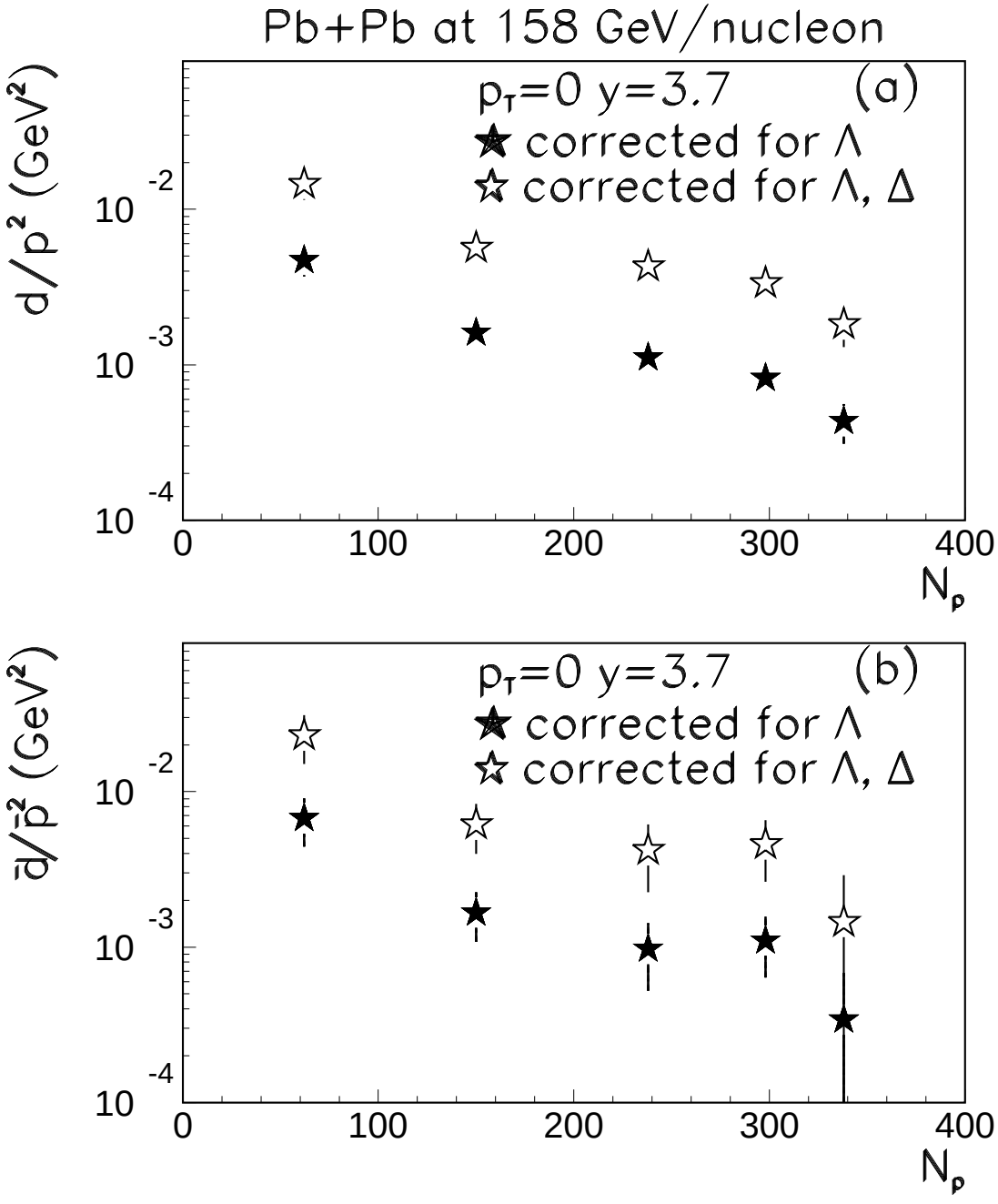

Figure 12. d/p^2 and $\overline{d}/\overline{p}^2$ invariant differential yield ratios in Pb+Pb collisions at 158 A GeV as a function of the number of participant nucleons N_p. The decay corrections were performed using [16].

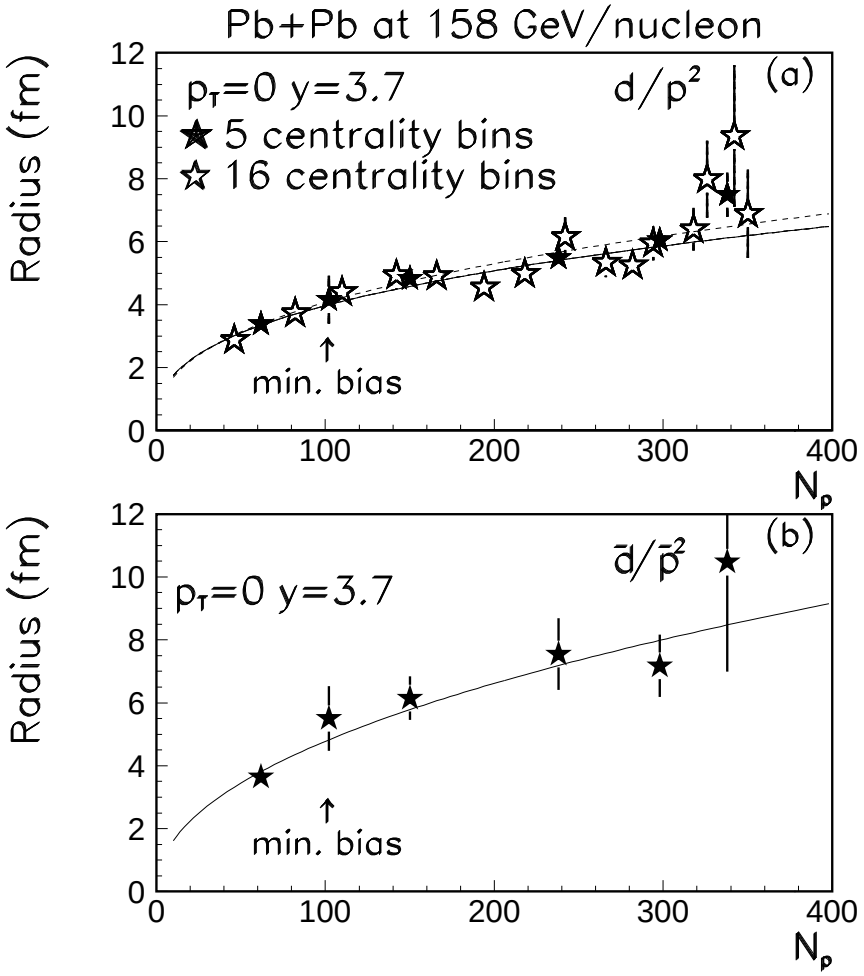

Figure 13. The source radius extracted from d/p^2 (a) and $\overline{d}/\overline{p}^2$ (b) yield ratios at y=3.7 and near zero p_T, as a function of the mean number of participant nucleons in Pb+Pb collisions at 158 A GeV. In (a) the results using 16 centrality bins are also shown as open points. The closed star points at $N_p \sim 103$ are extracted from the minimum bias Pb+Pb data sample. The radii were extracted using the model [25]. The diplayed curves are the results of the fit of the function $R \sim N_p^{\alpha}$ (see table 6 for the results).

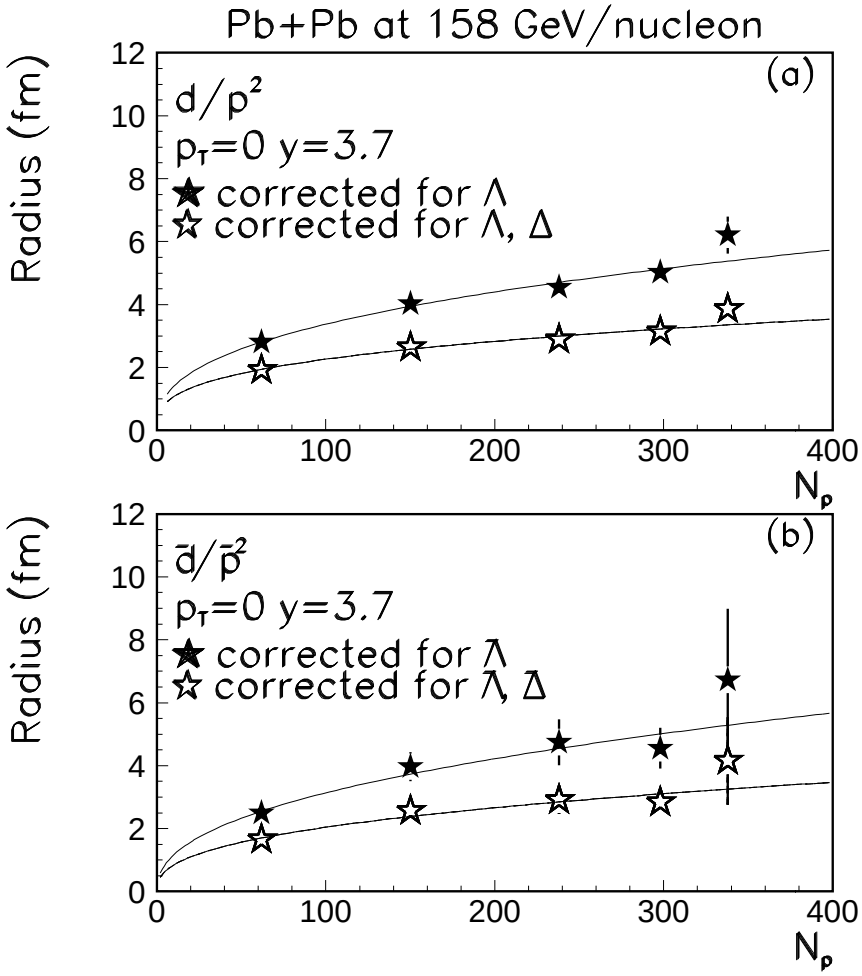

Figure 14. The source radius extracted from d/p^2 (a) and $\overline{d}/\overline{p}^2$ (b) yield ratios at y=3.7 and near zero p_T as a function of the mean number of participant nucleons in Pb+Pb collisions at 158 A GeV. The radii were extracted using the model [25]. The radii are corrected for $p, \overline{p}$ originating from Λ and Δ decays using the event generator VENUS 4.12 [16]. The displayed curves are the results of the fit of the function $R \sim N_p^{\alpha}$ (see table 6 for the results).

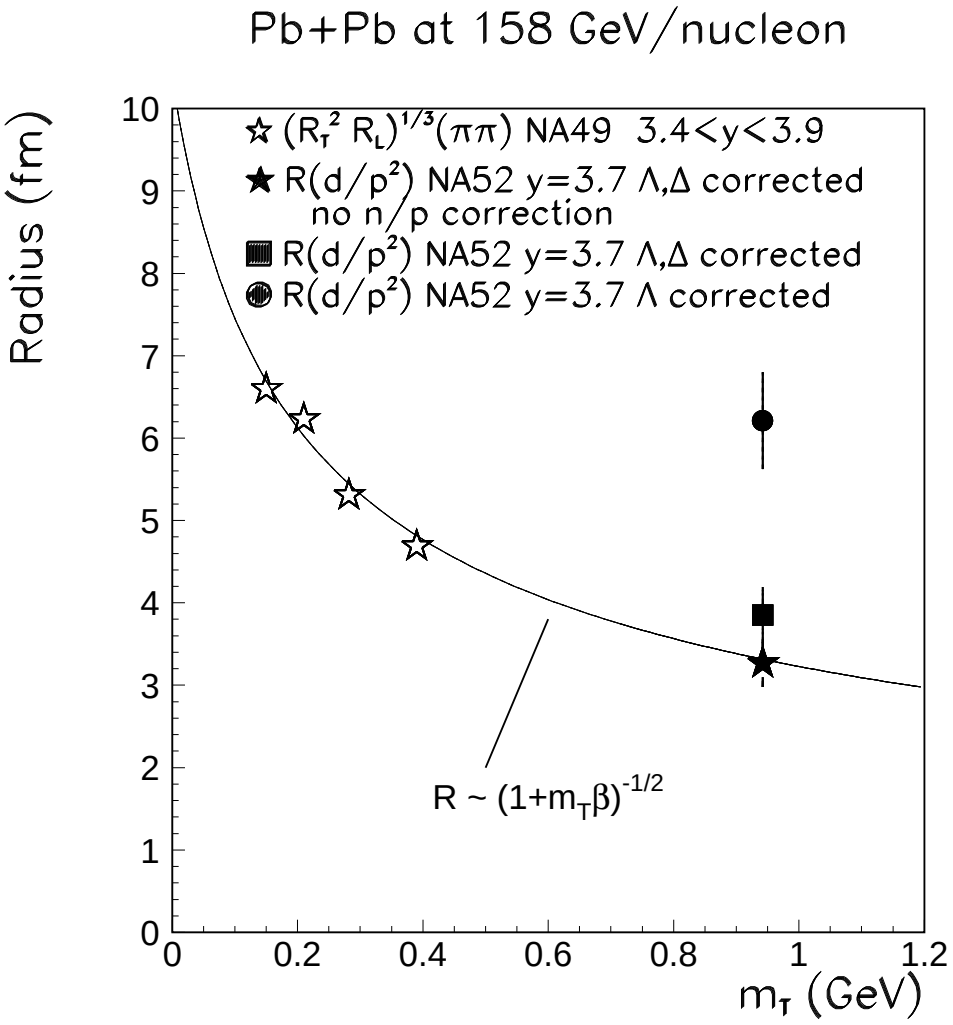

Figure 15. Transverse mass ($m_T = \sqrt{p_T^2 + m^2}$) dependence of the source radii extracted from d/p^2 at y=3.7 (full points, NA52 experiment) and of those extracted from $\pi\pi$-correlations [42] at 3.4< y <3.9 (open points, NA49 experiment) in Pb+Pb collisions at 158 GeV per nucleon. Both measurements were performed at similar centrality. The full star point shows the radius from d/p^2 without the correction for the excess of neutrons over protons in the lead nucleus. The displayed curve is a fit of the shown function to the open and closed stars. The results of the fit are $R = (10.4 \pm 0.79)(1 + m_T(9.3 \pm 2.3))^{-\frac{1}{2}}$ fm, with χ^2/DOF=0.8.